

See discussions, stats, and author profiles for this publication at: <https://www.researchgate.net/publication/255812246>

# Inelastic neutron scattering, Raman and DFT investigations of the adsorption of phenanthrenequinone on onion-like carbon

ARTICLE *in* CARBON · FEBRUARY 2013

Impact Factor: 6.2 · DOI: 10.1016/j.carbon.2012.09.016

---

CITATIONS

7

---

READS

30

## 7 AUTHORS, INCLUDING:



[Daniela Anjos](#)

Lam Research Corporation

15 PUBLICATIONS 392 CITATIONS

SEE PROFILE



[Alexander I Kolesnikov](#)

Oak Ridge National Laboratory

245 PUBLICATIONS 2,295 CITATIONS

SEE PROFILE

Available at [www.sciencedirect.com](http://www.sciencedirect.com)

SciVerse ScienceDirect

journal homepage: [www.elsevier.com/locate/carbon](http://www.elsevier.com/locate/carbon)

# Inelastic neutron scattering, Raman and DFT investigations of the adsorption of phenanthrenequinone on onion-like carbon

Daniela M. Anjos<sup>a</sup>, Alexander I. Kolesnikov<sup>a</sup>, Zili Wu<sup>a</sup>, Yu Cai<sup>b</sup>, Matthew Neurock<sup>b</sup>, Gilbert M. Brown<sup>a</sup>, Steven H. Overbury<sup>a,\*</sup>

<sup>a</sup> Oak Ridge National Laboratory, Oak Ridge, TN 37831, United States

<sup>b</sup> Department of Chemical Engineering, University of Virginia, Charlottesville, VA 22904, United States

## ARTICLE INFO

### Article history:

Received 23 May 2012

Accepted 7 September 2012

Available online 17 September 2012

## ABSTRACT

The orientation and bonding of adsorbed 9,10-phenanthrenequinone (PQ) on onion-like carbon (OLC) were determined by combining spectroscopy and density functional theory (DFT) calculations. Electrochemical measurements demonstrated relatively strong bonding of PQ to the OLC as indicated by persistent and reversible features in the cyclic voltammetry. Spectra of bulk solid and adsorbed PQ were obtained by inelastic neutron scattering (INS) and Raman spectroscopy, and the bands were compared with vibrational energies calculated from DFT. At energy losses (frequencies) above 400 cm<sup>-1</sup>, no band shifts in INS or Raman spectra were observed between bulk solid and adsorbed PQ. However, adsorption of PQ resulted in shifts in the lowest frequency modes (<400 cm<sup>-1</sup>), compared to crystalline PQ, which could only be identified by INS. DFT calculations also provided adsorption energies and from these and comparison of computed and experimental spectra it is determined that the molecule adsorbs parallel to the onion-like carbon surface through  $\pi$ - $\pi$  stacking interaction.

© 2012 Elsevier Ltd. All rights reserved.

## 1. Introduction

There is increasing interest in designing and improving new carbon materials for energy applications [1]. The performance of these materials has been improved over the years by functionalizing the carbon through chemical, electrochemical and thermal treatment [2–3]. Functionalization by adsorption of organic molecules on well defined surfaces including graphite and the resulting effects upon structural and electronic properties have been investigated for applications in electronic devices [4]. Understanding multi-electron and proton transfer to molecules attached to the carbon at a fluid–solid interface is crucial to controlling oxidation–reduction reactions at electrode and catalytic surfaces [5]. Quinones are often used

to functionalize carbon and are known to improve the activity of energy conversion and storage devices [6–8]. A complete understanding of the reactivity and thermodynamic properties of quinones (Q) and their reduced forms, the semiquinones (HQ<sup>-</sup>), quinhydrone (QHHQ), and hydroquinones (H<sub>2</sub>Q), is necessary to control proton coupled electron transfer reactions that occur during their oxidation–reduction reactions at electrode surfaces.

The adsorption of quinones and other aromatic molecules on flat graphene surfaces has been investigated on highly oriented pyrolytic graphite (HOPG) and pyrolytic graphite (PG) [9–11]. HOPG is the most ordered three dimensional graphite material [12]. PG has a lower degree of order and contains structural defects on the basal plane. These defects

\* Corresponding author.

E-mail address: [overburys@ornl.gov](mailto:overburys@ornl.gov) (S.H. Overbury).

0008-6223/\$ - see front matter © 2012 Elsevier Ltd. All rights reserved.

<http://dx.doi.org/10.1016/j.carbon.2012.09.016>

are more reactive than the relatively inert, well-ordered basal-plane regions, which often leads to the presence of a variety of chemical sites including oxo, acid and hydroxyl terminations. These chemical sites are believed to be more reactive for adsorption [3]. There is also evidence that the adsorption of quinones is affected by partial electronic charges on the basal plane of HOPG with induced defects [11]. The electronic perturbations near step edges lead to partial charges on HOPG that increase the electrostatic interaction with adsorbed quinones. These electrostatic interactions may be more important than dispersive interactions, hydrophobic effects or adsorption at specific chemical sites. In the present work we extend such investigations by probing how a quinone (9,10-phenanthrenequinone – PQ) is adsorbed on onion-like carbon (OLC), since this system shows promising results for application for supercapacitor and energy storage [13]. OLC is a highly specialized form of carbon with average particle size of about 6 nm, surface area of 500 m<sup>2</sup>/g and graphitic surface properties [1,14]. Concentric graphitic shells have been observed by TEM [14]. The extreme conditions under which OLC is prepared enable the formation of a clean graphite-type surface.

It is challenging to describe the interaction of aromatic molecules on chemically inert surfaces such as graphene. These interactions are usually through non-covalently bonded, dispersive interactions. If the molecules are large it is possible that the accumulative dispersive interaction can lead to strengthened adsorption [15]. In addition, when the adsorption occurs with the aromatic ring parallel to graphite surface, the molecular structure of the adsorbate can be very similar to that of an isolated gas phase molecule, and the distinction of both species becomes even more difficult [4]. Identification of adsorbed molecular species and their adsorption configuration is accessible from vibrational spectroscopy including IR absorption, Raman scattering and inelastic neutron scattering (INS). INS is particularly useful in providing information about hydrogen containing materials and their vibrational modes over a wide range of frequencies. The intensities of bands in INS depend on the neutron scattering cross-sections of the nuclei participating in a given mode, their vibrational amplitudes and the momentum transfer [16]. Because the neutron scattering cross-section of <sup>1</sup>H nuclei dominates relative to other nuclei, only modes in which H atoms contribute are observed in INS spectra [17]. Moreover, Raman and infrared spectra obey dipole selection rules while in INS all transitions are allowed, subject to the contribution of H motion to the mode. In this work, we used Raman, INS, cyclic voltammetry (CV) and density functional theory calculations to probe the adsorption of PQ on the surface of OLC.

## 2. Methods

Plates of HOPG and PG were obtained for use as electrodes. PG, grade PG-SN was obtained as plates (0.1875"H × 2"W × 2"L,) from the Graphitestore.com, cut to size with a diamond saw, and fresh basal plane surfaces were obtained by cleaving with a razor blade before use. HOPG (irregular sized scraps of Union Carbide ZYA Grade) was obtained from Union Carbide. A freshly cleaved basal plane surface was obtained by pressing

a piece of adhesive tape to the surface and removing a thin layer. A glassy carbon electrode (6 mm diameter) was obtained from Tokai Carbon. The OLC powder was prepared by annealing of carbon nanodiamonds according to procedures described previously [1]. Commercial 9,10-phenanthrenequinone or C<sub>14</sub>H<sub>8</sub>O<sub>2</sub> (PQ) with a purity of 95% was obtained from Aldrich and used without further purification.

In order to avoid the large number of defects near the edges of the electrodes, the electrochemical measurements were done by masking all but a 2 mm circle in the center, and the current density obtained by CV is calculated considering this exposed area. The PQ was adsorbed on the PG or HOPG carbon electrodes by soaking them in a methanol solution of PQ (5 × 10<sup>−3</sup> mol/L) for 20 min, and thoroughly rinsing the electrode with water. PQ coverage was calculated by the cathodic charge obtained by CV. PG and HOPG electrodes modified in this way were also used for *ex situ* Raman measurements.

The PQ-modified OLC prepared for CV, Raman and INS characterization, was obtained by similarly soaking the OLC in a PQ solution. The dispersion of OLC in PQ solution was sonicated for 20 min and then filtered using a PTFE (Teflon) filter 0.2 μm. The wet carbon was thoroughly rinsed with water and then dried overnight on a vacuum line at 60 °C. Dried PQ-modified OLC was sealed under air into Al sample boxes for INS measurements or placed on a sample stage for Raman measurements. Thermal gravimetric analysis (TGA) was used to determine the weight loading of PQ on the OLC as described previously [18] and using the published surface area of the OLC (500 m<sup>2</sup>/g), [1] the coverage of PQ was estimated to be 0.60 molecules/nm<sup>2</sup>. For electrochemical measurements, a weighed amount of PQ-treated OLC was re-dispersed in a measured volume water and sonicated to prepare a known, homogenous concentration of OLC. A drop of this dispersion was deposited on the top of a glassy carbon electrode and dried at room temperature in air. From the volume of the drop (and therefore the weight of OLC), and the surface area of the OLC, the total surface area of OLC on the glassy carbon electrode was calculated. The CV experiment was done in 1 mol/L H<sub>2</sub>SO<sub>4</sub>.

For Raman measurements a laser excitation at 244 nm (second-harmonic generation (SHG) from an Ar ion laser (Coherent, MotorFred I300C) with fundamental at 488 nm) was chosen to obtain resonance Raman spectra from adsorbed PQ molecules since they give strong electronic absorption in the deep UV region. The laser power at the sample was ca. 2 mW and the sample (electrode or PQ-modified OLC) was placed in air on an XY stage (Prior Scientific, OptiScan XY system), which translates in raster mode while collecting the spectra. The fast translation has been shown to minimize or eliminate laser damage to the samples. Cyclohexane solution was used as a standard for the calibration of the Raman shifts. Details about the Raman instrumentation are published elsewhere [19].

Inelastic neutron scattering data were collected at a temperature near 8 K for bulk PQ, OLC and PQ adsorbed on OLC. The experiments were done using the fine energy resolution spectrometer SEQUOIA at the ORNL Spallation Neutron Source [20]. SEQUOIA is a direct geometry time-of-flight spectrometer with variable energies of incident neutrons, from 10

to 2000 meV. To get the best energy resolution of  $\Delta E/E_i = 1\text{--}3\%$  at energy transfer of interest, we measured the INS spectra with three different incident energies of  $E_i = 60$ , 220 and 600 meV selected by the Fermi chopper that was rotating at 420 Hz for  $E_i = 60$  meV and 600 Hz for other energies. The data were recorded over a wide range of scattering angles, from  $-30^\circ$  to  $+60^\circ$  in horizontal plane and  $\pm 18^\circ$  in vertical directions. The background spectra for the empty container were measured under the same conditions and subtracted from the original data. Prior to further treatment, the collected neutron scattering data were transformed from the time-of-flight and instrument coordinates to the dynamical structure factor  $S(Q, E)$  and then to generalized vibrational density of states,

$$G(E) = S(Q, E) \cdot E \cdot \exp(u_H^2 Q^2) / \{Q^2 [n(E, T) + 1]\},$$

where  $n(E, T) = 1/[\exp(E/k_B T) - 1]$  is the population Bose factor. The value of  $u_H^2 = 0.019 \text{ \AA}^2$  was taken from fitting the  $Q$ -dependences of the dynamical structure factor peaks in the range around 100 meV, which were described as peaks originated due to one and two-phonon scattering processes by using the equation  $I(Q) = (a \cdot Q^2 + b \cdot Q^4) \exp(-u_H^2 Q^2)$ . For direct comparison with Raman spectra, the observed peak energy transfers were converted to  $\text{cm}^{-1}$  in the Figures ( $1 \text{ meV} \approx 8.06 \text{ cm}^{-1}$ ).

First principle plane wave density functional theory (DFT) calculations were carried out within the Generalized Gradient Approximation using the Vienna Ab Initio Simulation Package (VASP).<sup>[21–24]</sup> The dispersion correction is included using Grimme's DFT-D2 method. The Perdew–Wang 91 (PW91) form of the generalized gradient approximation was used to determine the corrections to exchange and correlation energies.

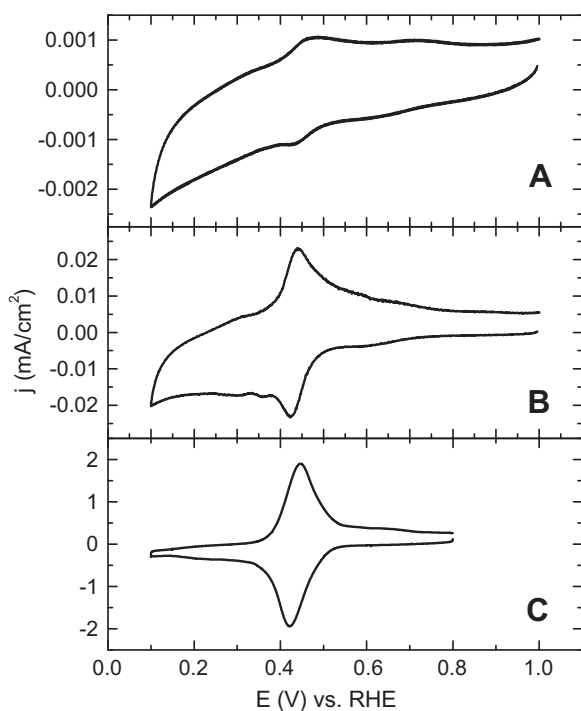


**Fig. 1** – Cyclic voltammograms of adsorbed PQ on (A) HOPG; (B) PG and (C) OLC. Electrolyte: 1.0 mol/L  $\text{H}_2\text{SO}_4$ . Scan rate: 20 mV/s.

Electron-ion interactions were described by using ultrasoft pseudopotentials.<sup>[25]</sup> The single-electron Kohn–Sham wave functions were described by planewave basis set expansion out to a cutoff energy 400 eV. The surface Brillouin zone is sampled using the  $3 \times 3 \times 1$  Monkhorst–Pack mesh. The electronic structure was converged to within a tolerance of  $1 \times 10^{-4}$  eV. Model surfaces used in calculations included a perfect graphene surfaces with a  $(7 \times 7)$  unit cell including 98 carbon atoms and a  $\text{C}_{720}$  fullerene used as a simplified model for OLC. All the atoms in the adsorbate and substrate were allowed to relax in the geometry optimizations until the forces are smaller than 0.02 eV/Å.

The vibrational spectra of adsorbed PQ and bulk crystalline PQ were also calculated using VASP. In these calculations the self-consistent field convergence is increased to  $10^{-6}$  eV to

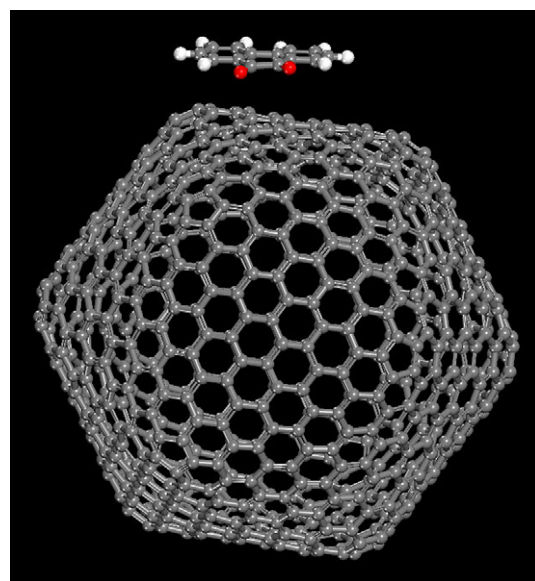


**Fig. 2** – DFT optimized structure for PQ adsorption on  $\text{C}_{720}$  fullerene.

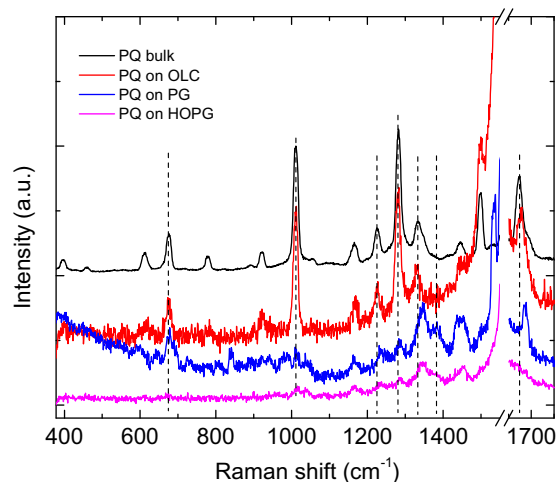


**Fig. 3** – Raman spectra using excitation at 244 nm for bulk PQ and for PQ adsorbed on the OLC or on the PG and HOPG electrodes. Dashed lines are added to guide the eye through key features.

obtain accurate force constants. Normal modes of vibrations were obtained from a Hessian matrix within the harmonic approximation. The Hessian matrix was constructed from single point energy calculations on 6N structures generated from the optimized structure by displacing each of the N atoms in three dimensions by  $\pm 0.02$  Å. Intensities for comparison with neutron scattering spectra were calculated using the eigenvectors  $e_j(E_j)$  for vibrational modes (j) of hydrogen atoms,

$$G_{\text{calc}}(E) = \sum |e_j(E_j)|^2 \delta(E - E_j).$$

Not knowing precisely the crystallographic structure of the bulk PQ used in our experiments, a stacking based upon the Cc structure of  $\beta$ -9,10-phenanthrenequinone polymorph described previously (in Fig. 3 of Rae et al. [26]) was used. The unit cell for bulk PQ crystal structure has  $a = 1$  nm,  $b = 1.0$  nm,  $c = 1.5$  nm,  $\alpha = 90^\circ$ ,  $\beta = 90^\circ$ ,  $\gamma = 90^\circ$  and includes four PQ molecules.

### 3. Results and discussion

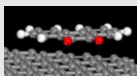
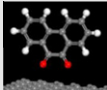
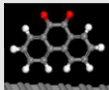
Fig. 1 shows CV curves obtained for PQ adsorbed on the basal planes of HOPG and PG and on the glassy carbon electrode with the PQ soaked OLC. The redox peak for quinone-hydroquinone is at 0.45 V vs. reversible hydrogen electrode (RHE) for all three electrodes. From the total amount of charge transferred, obtained by integrating the cathodic waves of the CVs, and assuming that each PQ molecule undergoes a  $2e^-$  transfer, the measured surface redox charge densities correspond to 14, 0.2 and  $4.1 \times 10^{-11}$  mol/cm<sup>2</sup> for the PG, HOPG, and OLC electrodes, respectively. These charge densities are obtained assuming the geometric area of the PG and HOPG electrodes and the surface area of the OLC as described above, and they correspond to surface PQ coverages of 0.84, 0.012 and 0.24 molecules/nm<sup>2</sup> for the PG, HOPG and OLC surfaces, respectively. Since a small amount of OLC was observed to wash off of the glassy carbon electrode during preparation, the measured charge density provides a lower limit of the PQ coverage on the OLC. A CV of freshly cleaved PG electrode (not shown in Fig. 1) exhibited native peaks at around 0.6 V vs. RHE related to oxygen functional groups at the carbon surface. Traces of these native groups are weakly contributing to the CVs of PQ on HOPG (Fig. 1A) and on PG (Fig. 1B) but are not visible in the CV of the OLC indicating the low concentrations of these chemical sites on the OLC. The CV curves were reproducible and could be repeated without obvious change for many cycles. The shape of the CV curve and the clearly defined waves demonstrate that the PQ is adsorbed on the

surface and is held strongly enough that extended exposure to the aqueous, acid electrolyte does not remove it from the surface.

Density functional theory with dispersion corrections (DFT-D) was used to compute the adsorption binding energy of PQ on a flat, defect-free graphene surface. The calculation was performed for PQ in three different orientations in which the plane of the PQ molecules lie (1) parallel to the surface, (2) perpendicular to the surface with O atoms toward the surface or (3) perpendicular to the surface with O atoms away from the surface. The calculations indicate that the most stable PQ adsorption on the perfect graphene surface is in the parallel,  $\pi$ -bonded orientation. The computed adsorption energy for this  $\pi$ -bound mode is  $-1.08$  eV and the separation distance between PQ molecular plane and graphene surface is 0.34 nm. As shown in Table 1 the parallel orientation is more stable than the perpendicular O-up configuration by 0.47 eV. The carbon onion surface differs from a flat, perfect graphene surface in that it has defects and curvature that might be expected to affect adsorption energy. Similar to the graphene surface, it is expected to have a very low concentration of native, functional groups. To judge curvature effects, PQ adsorption on a C<sub>720</sub> fullerene (with 2.5 nm diameter) was also calculated. The optimized structure of the fullerene and the adsorbed PQ are illustrated in Fig. 2. Positive (convex) curvature might be expected to decrease the adsorption energy of a molecule bonded by dispersive interactions due to decreased overlap. In agreement, the PQ adsorption energy on the C<sub>720</sub> fullerene is  $-0.86$  eV, slightly weaker than on perfect, flat graphene. The OLC used in the experiments had average 6 nm diameter and would therefore have on average less curvature and be more like the graphene surface in terms of quinone adsorption.

Spectroscopy of adsorbed PQ was used to compare with the computational results. In Fig. 3 Raman spectra for PQ adsorbed on OLC, HOPG, and PG are compared with the spectrum of bulk, solid PQ. The spectra of the carbon surfaces are dominated by the G band, expected near  $1581$  cm<sup>-1</sup> for HOPG and PG, [27] nearly matching the most intense mode for PQ at  $1592$  cm<sup>-1</sup> due to the aromatic C=C stretch. Sharp peaks due to vibrational modes of bulk or adsorbed PQ are observed above and below the G peak. Positions of all Raman peaks observed between 400 and  $1800$  cm<sup>-1</sup> are summarized in Table 2. In the range investigated, no frequency shifts were detected for PQ adsorbed on carbon onion compared with bulk PQ. In contrast, frequency shifts were observed for PQ adsorbed on HOPG and PG. Significant differences in relative peak intensities are also observed for the case of adsorption

**Table 1 – PQ adsorption energies (eV) on model graphene surfaces in three orientations. The model surface coverage is 0.39 molecules/nm<sup>2</sup>. The carbon atoms are in gray, oxygen in red, and hydrogen in white.**

Quinone orientation	Parallel	Perpendicular O-atoms down	Perpendicular O-atoms up
PQ E(ads)	-1.08	-0.41	-0.61
			



**Table 2 – Observed Raman vibrational frequencies and INS energy losses (in  $\text{cm}^{-1}$ ) from bulk PQ and PQ adsorbed on OLC (400–1800  $\text{cm}^{-1}$ ).**

Raman		INS		Assignment [33]
PQ bulk	PQ <sub>ads</sub> OLC	PQ bulk	PQ <sub>ads</sub> OLC	
398	n/o	403	401	C–H o–p bend
434 w	n/o	418	418	
n/o	n/o	437	437	
458	n/o	n/o	464	
n/o	n/o	550	554	
612	622	617	617	C–H o–p bend
675	673	674	n/o	
717 w	n/o	714	714	
780	780	778	770	
820 w	n/o	827	827	
890 w	899	892	886	C=C i–p bend
920	921	n/o	n/o	
n/o	n/o	971	968	
n/o	n/o	1003	987	
1012	1012	n/o	n/o	
1055	1055 w	1050	1050	C–H i–p bend
n/o	n/o	1092	1101	
1104 w,br	n/o	1125	1125	C–H i–p bend
1165	1169	1165	1165	
1226	1226	1230	1230	C=C stretch
1283	1283	1282	1282	C=C stretch
1334	1334	1336	1336	C=C stretch + C–O bend
1414 w	n/o	1448	1448	C=C stretch
1446	1447	1479	1479	
1499	1499	1506	1501	C=C stretch
1592	1592 br	1602	1593	C=C stretch; G band
n/o	n/o	n/o	1653	C=O asym. stretch
1674	1674	n/o	n/o	C=O sym. stretch

\* n/o = not observed; w = weak; br = broad, o–p = out-of-plane; i–p. = in-plane.

of PQ on PG and HOPG compared to the adsorption of PQ on OLC and bulk PQ. For instance, the bands at  $\sim 1012 \text{ cm}^{-1}$  (in-plane C=C stretch, or ring breathing mode) and  $1283 \text{ cm}^{-1}$  (C=C stretch), which are very prominent in bulk PQ and for PQ on OLC, have lower intensities after adsorption on PG and HOPG. Additionally, the band near  $1334 \text{ cm}^{-1}$ , for bulk PQ and PQ on OLC, assigned to mixture of C=C stretching and neighboring C–O symmetric bending modes, are blue-shifted at least  $10 \text{ cm}^{-1}$ , for PQ on PG and HOPG and a new peak is apparent at  $1382 \text{ cm}^{-1}$ . The latter peak is not present in bulk PQ or in the spectra of the untreated (PQ-free) HOPG and PG surfaces (not shown). It is expected that oxo-groups present on the HOPG and PG may interact with and affect the orientation of adsorbed PQ. This interaction could be stronger and covalent and may explain the changes in the Raman spectra of adsorbed PQ on these surfaces. Finally, a shoulder at  $1550 \text{ cm}^{-1}$  visible in Fig. 3 for the PQ adsorbed on PG is due to incidental molecular, gas phase  $\text{O}_2$  present in the Raman setup. It was also observed in the spectrum of bare PG, absent any PQ (not shown).

The INS and calculated spectra at the same frequency range as for the Raman are shown in Fig. 4A and B, respectively. The INS spectra using 220 meV incident neutrons are shown in Fig. 4A for OLC, for adsorbed PQ on OLC (PQ<sub>ads</sub>) and for bulk PQ. Alignment with many Raman features is found in Table 2, but a different number of bands are detected in INS compared to Raman. Dipole selection rules are not

applicable for INS and so bands forbidden in Raman may be observed in INS. But neutrons are quite insensitive to modes that do not involve hydrogen motions, so in particular the localized C=O stretch ( $1674 \text{ cm}^{-1}$ ) and the C=C in-plane stretch ( $1012 \text{ cm}^{-1}$ ) that are strong in the Raman spectra are weak and not observed in the INS spectrum. Identically to the Raman results, there are essentially no shifts in energy observed for the bands detected for PQ on OLC when compared with bulk PQ. The INS spectra for OLC without adsorbed PQ, does not exhibit such sharp features, although some weak broad bands are apparent. The absence of sharp features on the (PQ-free) OLC indicates that the sharp modes observed for the PQ-modified OLC are all associated with the adsorbed PQ. INS spectra predicted for the DFT-optimized structures (Table 1) are shown in Fig. 4B. In addition, the bulk crystallographic structure described above was used as a structural model to compute the spectrum for bulk PQ. In this spectral range, only a small distinction is observed between parallel and perpendicular PQ orientations, around  $900\text{--}1000 \text{ cm}^{-1}$ . The DFT-calculated spectra in Fig. 4B are in good agreement with the experimental results obtained by INS.

The INS spectra using higher energy neutrons (600 meV) and calculated spectra for the same range of energy are shown in Fig. 5, providing information up to  $3500 \text{ cm}^{-1}$ . The only peak detected at the range is present at  $3050 \text{ cm}^{-1}$  due to C–H stretching modes. This peak is strong for PQ on OLC and for neat PQ but is not present on unmodified OLC. The

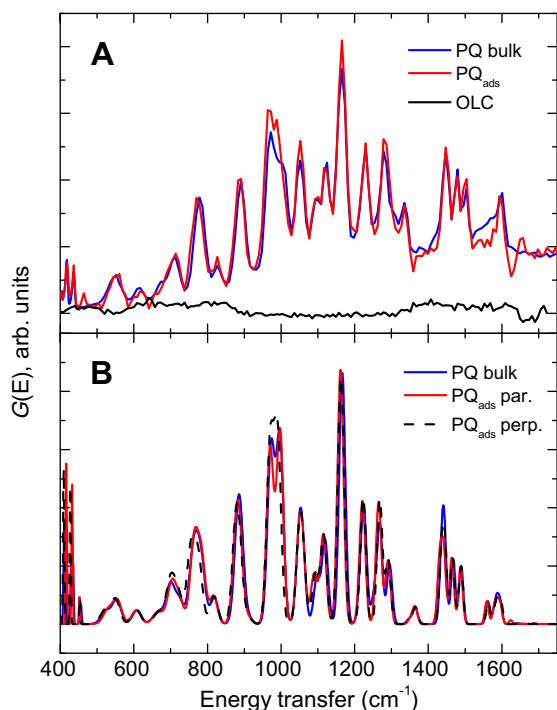


**Fig. 4 – (A)** Experimental spectra obtained by inelastic neutron scattering with  $E_i = 220$  meV. Intensity of PQ bulk is divided by 10. **(B)** Calculated spectra of bulk PQ and of PQ adsorbed parallel to the surface (PQ<sub>ads</sub> par.) and perpendicular to the surface with the O atoms up (PQ<sub>ads</sub> perp.).

absence of this peak in the unmodified OLC demonstrates that this material is virtually free of C–H terminations.

At lower incident neutron energy, 60 meV, INS permits observation of very low frequency modes below 400 cm<sup>-1</sup>. This energy range produced some of the clearest indications of the effect of bonding on the surface of the OLC as shown by comparison of bulk PQ with PQ adsorbed on OLC in Fig. 6A. The frequencies of the features observed below 400 cm<sup>-1</sup> are compared in Table 3. We were unable to find IR or Raman spectroscopic data in the literature of this low frequency range for the PQ molecule, but based upon molecular *phenanthrene* and our DFT calculations, these low energy bands may be generally assigned to torsion and deformation modes within the molecule, as well as inter-molecular translational and librational vibrations of molecules. The calculated INS spectra in this energy range are shown for bulk PQ and PQ adsorbed parallel and perpendicular on graphene in Fig. 6B. The DFT-calculated spectrum for bulk PQ shown in Fig. 6B is in good agreement with the experimental results shown in Fig. 6A. Overall, shifts of the bands are observed when comparing calculated and experimental spectra at this low energy due in part to difficulties with acoustic modes that are not well described in the simulations. In addition, simulations of other stacking of the bulk PQ, besides the crystallographic structure described above, led to variation of the features below 150 cm<sup>-1</sup> indicating the sensitivity of these features to inter-molecular interactions. According to the DFT calculations, PQ adsorbed in the parallel orientation is

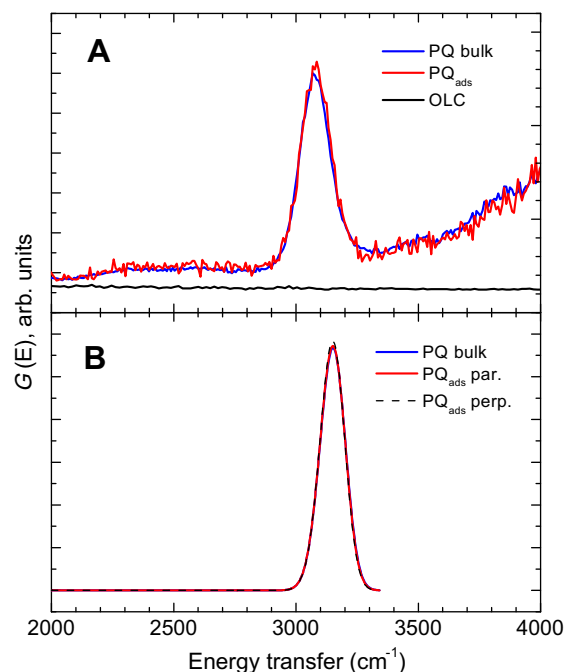


**Fig. 5 – (A)** Experimental spectra obtained by inelastic neutron scattering with  $E_i = 600$  meV. Intensity of PQ bulk is divided by 10. **(B)** Calculated spectra of bulk PQ and PQ adsorbed parallel to the surface (PQ<sub>ads</sub> par.) and perpendicular to the surface with the O atoms up (PQ<sub>ads</sub> perp.).

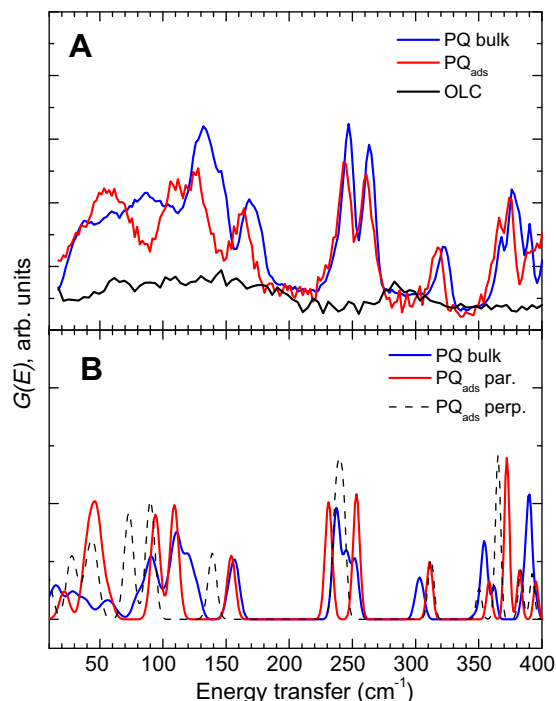


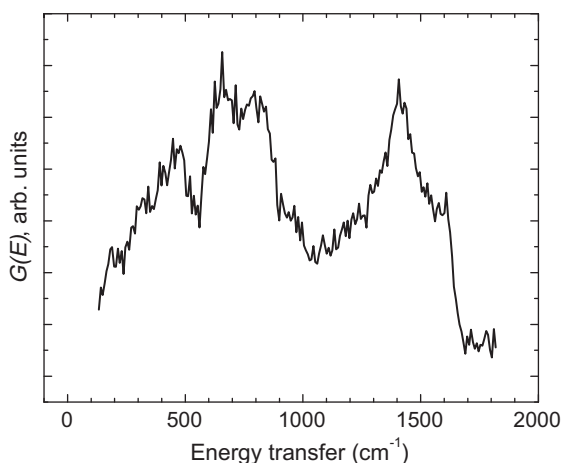
**Fig. 6 – (A)** Experimental spectra obtained by inelastic neutron scattering with  $E_i = 60$  meV. Intensity of PQ bulk is divided by 10. **(B)** Calculated spectra of bulk PQ and PQ adsorbed parallel to the surface (PQ<sub>ads</sub> par.) and perpendicular to the surface with the O atoms up (PQ<sub>ads</sub> perp.).

**Table 3 – Vibrational assignments of INS spectra measured with  $E_i = 60$  meV.**

Observed frequency/cm <sup>-1</sup>	
PQ bulk	PQ <sub>ads</sub> on OLC
131	109
146	125
170	162
245	242
261	259
323	318
365	363
375	372

the most stable structure and the corresponding calculated spectrum looks more similar to the experimental spectrum for PQ adsorbed on OLC. In particular, the features around 100–130 cm<sup>-1</sup> and 230–270 cm<sup>-1</sup> agree best between the experimental spectrum and the spectrum computed for PQ<sub>ads</sub> in parallel orientation, and these discriminate against the perpendicular configuration.

In all energy ranges, the scattering features of the untreated OLC were of relatively low intensity, compared to those of the PQ and the PQ-modified OLC, and exhibited no sharp features. This is due to the low carbon neutron scattering cross section, and demonstrates that the amount of bonded H in the OLC is very small. The complete absence of a mode near 3050 cm<sup>-1</sup> or near 3500 cm<sup>-1</sup> in the OLC spectrum (Fig. 5A) demonstrates the absence of C–H and O–H terminations in the OLC. To explore this point further, an INS spectrum below 1800 cm<sup>-1</sup> from the OLC is shown in Fig. 7, obtained using incident neutron energies of 250 meV. It exhibits three broad bands (near 400, 600–900 and 1250–1650 cm<sup>-1</sup>) showing the behavior typical for the graphite type structures [28–30]. The lower frequency bands can be mostly assigned to out-of-plane acoustic and optic modes of carbon while the broad band from 1250–1650 can be assigned to in-plane longitudinal and transverse optical modes (due mostly to C–C stretching vibrations). In particular, bands are not seen at 860 or 1180 cm<sup>-1</sup> that have been reported to be due to C–H

**Fig. 7 – Experimental spectrum obtained by inelastic neutron scattering for OLC with  $E_i = 250$  meV.**

bending modes,[16] a further indication of the absence of any kind of C–H or O–H groups in the sample.

Results of the Raman and INS spectra indicate that the PQ is relatively unaffected by adsorption on the OLC surfaces or on the flat graphitic surfaces. This indicates that the PQ is not rehydridized or covalently bonded to the surface. Instead it suggests bonding through a  $\pi$ – $\pi$  stacking interactions. Most of the differences in the spectra of adsorbed and bulk PQ were found below 400 cm<sup>-1</sup>. By comparison with phenanthrene, these lowest frequencies bands are the result of out-of-plane ring deformations,  $\alpha$ (C–C–C) and changes in the endocyclic torsion angles  $\delta$ (C–C–C–C) [31–32]. Table 3 shows that for the frequencies lower than 400 cm<sup>-1</sup> the peaks for adsorbed PQ are shifted to lower frequency than for bulk PQ. Since  $\pi$  interaction is a major adsorptive force, it is expected that a ring deformation mode should be sensitive to the amount and direction of charge transfer and to the bonding strength between the molecule and the carbon surface. Two prominent modes observed for bulk PQ at 131 and 146 cm<sup>-1</sup> appear to be shifted lower to 109 and 125 cm<sup>-1</sup> for adsorbed PQ (Fig. 6A and Table 3). A previously published comparison of Raman with molecular dynamics calculations for the related aromatic molecule phenanthrene, [31] reveal two pronounced low frequency out-of-plane deformation modes described as twist and butterfly, and these are observed at 78 and 96 cm<sup>-1</sup>, respectively. Carbonyls on PQ might be expected to stiffen these torsion modes compared to phenanthrene, shifting them to higher frequencies. This expectation suggests that the two prominent peaks may be assigned to these modes.

The parallel adsorption configuration of the PQ molecule to the carbon surface implies that the carbonyl functional groups of the molecule may be relatively unrestricted in their ability to interact with water or solvent molecules at a fluid-carbon interface. In particular, reduction of the PQ to the semiquinone or the hydroquinone, and its reverse oxidation, may occur without impediment from its bonding to the surface. If instead, for example, the molecule were to bond to the carbon through the carbonyl, the redox process would be expected to be strongly affected. In addition, the fact that the molecule can bond relatively strongly, even at flat graphitic surface relatively free of defects, is consistent with the relatively high coverages observed by TGA and in the CV measurements and the reversibility and relative robustness of the adsorbate redox behavior.

## 4. Conclusion

Electrochemical measurements from phenanthrenequinone (PQ) adsorbed at an aqueous interface of planar or nanostructured onion-like carbon demonstrate a relatively strong bonding and reversible redox behavior. To understand the bonding of PQ to the carbon surfaces, INS and Raman spectra of bulk and adsorbed PQ were obtained and compared with DFT calculations. The results were also compared with adsorption of PQ on pyrolytic graphite (PG) and highly oriented pyrolytic graphite (HOPG). It is concluded that the PQ is bonded in a parallel orientation through  $\pi$  interactions between the molecules and the OLC based upon (1) absence of changes in the vibrational bands that would indicate covalent bonding and (2) comparison and agreement of the experimental INS



spectrum with the spectrum calculated for this bonding orientation. Adsorption of PQ results in changes of the torsional and out-of-plane ring deformation modes of the adsorbed molecule that are signaled by red-shifts in the lowest frequency modes (compared to crystalline PQ) and consistent with the parallel bonding configuration. Dispersive forces lead to attraction and adsorption energy near 1 eV as indicated by DFT-D calculations.

## Acknowledgements

This work was supported as part of the FIRST Center, an Energy Frontier Research Center funded by the U.S. Department of Energy, Office of Science, Office of Basic Energy Sciences. INS experiments at the Spallation Neutron Source and Raman measurements at Center for Nanophase Materials Sciences were supported by the Scientific User Facility Division, Office of Basic Energy Sciences, US Department of Energy. The authors wish to thank John McDonough and Yuri Gogotsi for providing the OLC and for useful discussions.

## REFERENCES

- [1] Pech D, Brunet M, Durou H, Huang P, Mochalin V, Gogotsi Y, et al. Ultrahigh-power micrometre-sized supercapacitors based on onion-like carbon. *Nat Nanotechnol* 2010;5(9):651–4.
- [2] Fantini C, Usrey ML, Strano MS. Investigation of electronic and vibrational properties of single-walled carbon nanotubes functionalized with diazonium salts. *J Phys Chem C* 2007;111(48):17941–6.
- [3] Wildgoose GG, Abiman P, Compton RG. Characterising chemical functionality on carbon surfaces. *J Mater Chem* 2009;19(28):4875–86.
- [4] Schmidt WG, Seino K, Preuss M, Hermann A, Ortmann F, Bechstedt F. Organic molecule adsorption on solid surfaces: chemical bonding, mutual polarisation and dispersion interaction. *Appl Phys A: Mater Sci Process* 2006;85(4):387–97.
- [5] Hammes-Schiffer S. Theory of proton-coupled electron transfer in energy conversion processes. *Acc Chem Res* 2009;42(12):1881–9.
- [6] Jang BZ, Liu CG, Neff D, Yu ZN, Wang MC, Xiong W, et al. Graphene surface-enabled lithium ion-exchanging cells: next-generation high-power energy storage devices. *Nano Lett* 2011;11(9):3785–91.
- [7] Sarapuu A, Helstein K, Vaik K, Schiffrin DJ, Tammeveski K. Electrocatalysis of oxygen reduction by quinones adsorbed on highly oriented pyrolytic graphite electrodes. *Electrochim Acta* 2010;55(22):6376–82.
- [8] Pognon G, Brousse T, Demarconnay L, Belanger D. Performance and stability of electrochemical capacitor based on anthraquinone modified activated carbon. *J Power Sources* 2011;196(8):4117–22.
- [9] Brown AP, Anson FC. Cyclic and differential pulse voltammetric behavior of reactants confined to the electrode surface. *Anal Chem* 1977;49(11):1589–95.
- [10] Kano K, Uno B. Surface-redox reaction mechanism of quinones adsorbed on basal-plane pyrolytic graphite electrodes. *Anal Chem* 1993;65:1088–93.
- [11] McDermott MT, McCreery RL. Scanning-tunneling-microscopy of ordered graphite and glassy-carbon surfaces – electronic control of quinone adsorption. *Langmuir* 1994;10(11):4307–14.
- [12] McCreery RL. Advanced carbon electrode materials for molecular electrochemistry. *Chem Rev* 2008;108(7):2646–87.
- [13] McDonough JK, Frolov AI, Presser V, Niu J, Miller CH, Ubieta T, et al. Influence of the structure of carbon onions on their electrochemical performance in supercapacitor electrodes. *Carbon* 2012;50:3298–309.
- [14] Portet C, Yushin G, Gogotsi Y. Electrochemical performance of carbon onions, nanodiamonds, carbon black and multiwalled nanotubes in electrical double layer capacitors. *Carbon* 2007;45(13):2511–8.
- [15] Grimme S. Do special noncovalent p–p stacking interactions really exist? *Angew Chem Int Ed* 2008;47:3430–4.
- [16] Lennon D, McNamara J, Phillips JR, Ibberson RM, Parker SF. An inelastic neutron scattering spectroscopic investigation of the adsorption of ethene and propene on carbon. *Phys Chem Chem Phys* 2000;2(19):4447–51.
- [17] Pawlukojc A, Natkaniec I, Bator G, Grech E, Sobczyk L. Inelastic neutron scattering studies on dichloro-1,4-benzoquinones. *Spectrochim Acta Part A Mol Biomol Spectrosc* 2004;60(12):2875–82.
- [18] Chathoth SM, Anjos DM, Mamontov E, Brown GM, Overbury SH. Dynamics of phenanthrenequinone on carbon nano-onion surfaces probed by quasielastic neutron scattering. *J Phys Chem B* 2012;116:7291–5.
- [19] Wu Z, Dai S, Overbury SH. Multiwavelength raman spectroscopic study of silica-supported vanadium oxide catalysts. *J Phys Chem* 2010;114:412–22.
- [20] Granroth GE, Kolesnikov AI, Sherline TE, Clancy JP, Ross KA, Ruff JPC, et al. SEQUOIA: a newly operating chopper spectrometer at the SNS. *J Phys: Conf Ser* 2010;251:012058.
- [21] Grimme S. Semiempirical GGA-type density functional constructed with a long-range dispersion correction. *J Comput Chem* 2006;27(15):1787–99.
- [22] Grimme S. Accurate description of van der Waals complexes by density functional theory including empirical corrections. *J Comput Chem* 2004;25(12):1463–73.
- [23] Kresse G, Furthmüller J. Efficient iterative schemes for ab initio total-energy calculations using a plane-wave basis set. *Phys Rev B* 1996;54(16):11169–86.
- [24] Kresse G, Furthmüller J. Efficiency of ab-initio total energy calculations for metals and semiconductors using a plane-wave basis set. *Comput Mater Sci* 1996;6(1):15–50.
- [25] Vanderbilt D. Soft self-consistent pseudopotentials in a generalized eigenvalue formalism. *Phys Rev B* 1990;41(11):7892–5.
- [26] Rae AD, Willis AC. 9,10 Phenanthrenequinone, not your average structure. *Z Kristallogr* 2003;218:221–30.
- [27] Dresselhaus MS, Jorio A, Hofmann SM, Dresselhaus G, Saito R. Perspectives on carbon nanotubes and graphene raman spectroscopy. *Nano Lett* 2010;10:751–8.
- [28] Mohr M, Maultzsch J, Dobardžić E, Reich S, Milošević I, Damnjanović M, et al. Phonon dispersion of graphite by inelastic X-ray scattering. *Phys Rev B* 2007;76(3):035439.
- [29] Wirtz L, Rubio A. The phonon dispersion of graphite revisited. *Solid State Commun* 2004;131(3–4):141–52.
- [30] Gospodarev IA, Kravchenko KV, Syrkina ES, Feodos'ev SB. Quasi-two-dimensional features in the phonon spectrum of graphite. *Low Temp Phys* 2009;35(7):589–95.
- [31] Zhigalko MV, Shishkin OV, Gorb L, Leszczynski J. Out-of-plane deformability of aromatic systems in naphthalene, anthracene and phenanthrene. *J Mol Struct* 2004;693(1–3): 153–9.
- [32] Godec J, Colombo L. Interpretation of the vibrational spectrum of crystalline phenanthrene. *J Chem Phys* 1976;65(11):4693–700.
- [33] Ishioka T, Uchida T, Teramae N. Time-resolved near-infrared surface-enhanced Raman spectroscopy of a surface-confined electrochemical reaction of 9,10-phenanthrenequinone. *Bull Chem Soc Jpn* 1999;72(12):2713–7.